Steady State Creep in Cu-Al Solid Solution Alloys at Intermediate Temperatures and Low Stresses

L. Kloc, J. Fiala and J. Cadek

Institute of Physical Metallurgy, Czechoslovak Academy of Sciences
616 62 Brno, Czechoslovakia

CONTENTS

Abstract

Creep in Cu-5Al and Cu-14Al solid solution alloys at homologous temperatures close to 0.6 and stresses lower than 5 MPa was investigated using the helicoid spring specimen technique. Both alloys exhibit Coble diffusional creep; however, a non-viscous mechanism was found to operate in parallel with that of Coble in the Cu-14Al alloy. The nature of the non-viscous creep mechanism is discussed and a possible explanation for the different behaviour of both alloys is presented.

1. Introduction

Contemporary demands on the creep lives of some important parts of thermal power-generating equipment can be met only if the creep rates of materials from which they are produced do not exceed $10^{-11}s^{-1}$. Thus the admissible stresses are necessarily low enough for specific low-stress creep mechanisms to operate in parallel with power law (recovery) creep or to even dominate it. This has quite naturally led to a realization of the significance to investigate such low stress creep mechanisms. In the past two decades, low stress creep has been studied almost exclusively in pure metals. In the present paper, some results of an investigation of creep in Cu-5Al and Cu-14Al solid solution alloys at low stresses and intermediate temperatures are reported and analyzed.

2. Experimental

The creep experiments were conducted in purified hydrogen using the helicoid spring specimen technique. The apparatus has been described in detail elsewhere /1/. The temperature along the specimen axis was uniform to within 1 K and was stabilized to within 1 K. The coil spacing increments were measured by means of a cathetometer with a sensitivity of ± 1 µm. With respect to the non-viscous creep behaviour of one of the alloys investigated, the evaluation of the stress dependence of creep rate was performed using a new numerical procedure /2/ that makes it possible to correct for redistribution of stress across the specimen wire cross section to be made.

Two alloys with different aluminium concentrations were investigated, namely alloy A with 4.9 at.%Al (2.14 wt.%Al) and alloy B with 14 at.%Al (6.5 wt.%Al). Helicoid spring specimens of mean coil diameters 19.21 mm and/or 26.97 mm were prepared in the usual way (see e.g. /1/) by winding the wire on a threaded stainless steel bolt and subsequently annealing in vacuum at various temperatures to obtain various grain sizes. After the vacuum anneal, the specimen surface was chemically polished.

The grain size was determined metallographically using the linear intercept method before as well as after the creep test. No grain growth during creep was detected.

3. Results

Altogether about 200 and 250 creep curves were obtained and analyzed for alloy A and B, respectively. All creep curves show that transient creep occurs, after which steady state commences. Typical examples of creep curves are illustrated in Fig. 1.

The stress dependences of steady state creep rate are clearly different for the two alloys. This can be seen in Figs. 2 and 3. While alloy A exhibits viscous behaviour at all applied stresses under consideration, alloy B exhibits viscous creep only at stresses lower than about 1 MPa. At higher stresses, a non-viscous creep mechanism obviously contributes to the measured creep rate in this alloy. In the case of non-viscous creep behaviour, the necessity of the correction for stress redistribution can be seen in Fig. 3. Thus, the steady state creep rate for alloy B should be considered as a sum of the rates contributed by the viscous and non-viscous creep mechanisms:

$$\dot{\varepsilon}_s = \dot{\varepsilon}_V + \dot{\varepsilon}_{NV} \qquad (1)$$

In Eq. 1 $\dot{\varepsilon}_V \propto (\delta - \delta_o)$ is the creep rate due to the viscous mechanism; $\dot{\varepsilon}_{NV} \propto \delta^n$ is the rate due to the viscous mechanism; δ is the applied stress; and δ_o is the threshold stress. In both alloys, small threshold stresses were found to be associated with the viscous creep mechanism. The threshold stress seems to be independent of temperature and grain size but a large scatter of

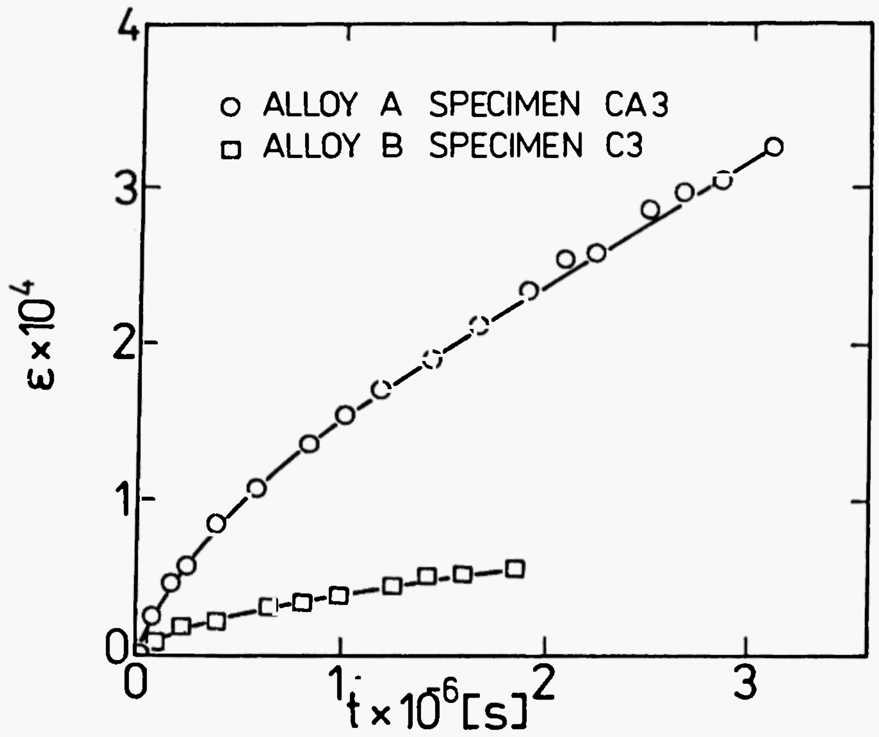

Fig. 1: Typical creep curves of both alloys. T = 773 K, δ = 1.1 MPa, L = 130 μm.

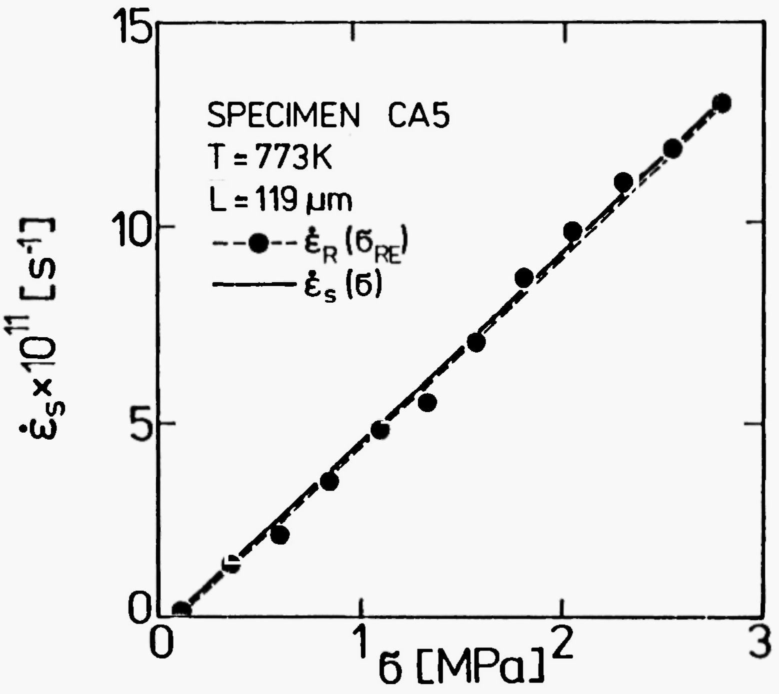

Fig. 2: Stress dependence of steady state creep rate for alloy A in double linear coordinates. In Figs. 2 and 3 ε_R are measured values of strain rate at various stresses δ_{RE} on the specimen wire surface; ε_s (δ) relation is calculated from ε_R and δ_{RE} data using a procedure described in /2/.

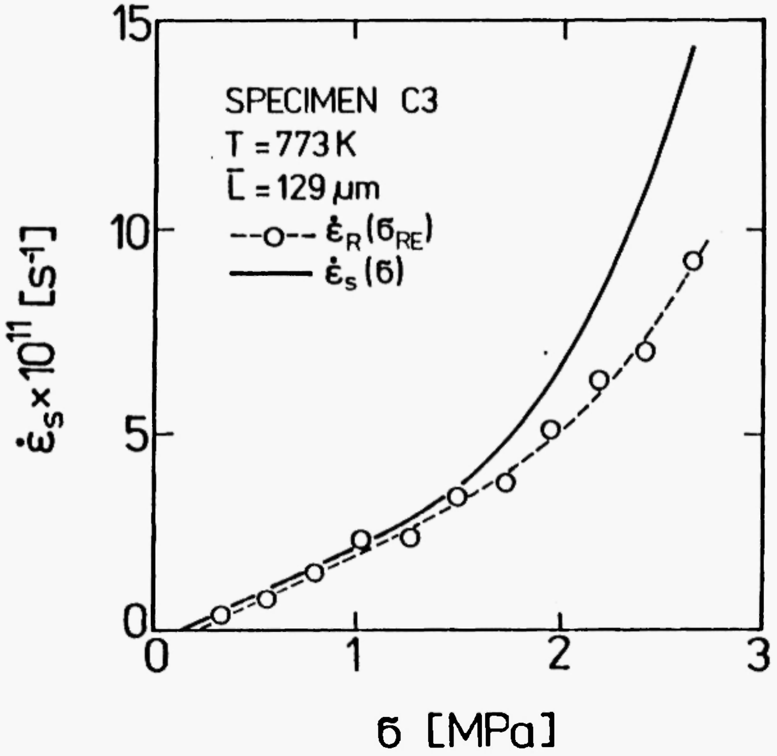

Fig. 3: Stress dependence of steady state creep rate for alloy B in double linear coordinates (c.f. caption of Fig. 2).

threshold stress values makes any definite conclusion impossible. The analysis of results shows that exponent n is approximately equal to 2.

In Fig. 4, grain size dependences of the stress normalized creep rates for both mechanisms are shown for alloy B. It is obvious that creep rates due to these mechanisms depends strongly on grain size; in fact, they are inversely proportional to the third power of the grain size.

The low stress steady state creep is frequently described by the phenomenological equation:

$$\varepsilon'_s = A\,\frac{dGb}{kT}\left(\frac{b}{d}\right)^g\left(\frac{\delta-\delta_o}{G}\right)^n \qquad (2)$$

where A is the dimensionless constant, D the effective diffusion coefficient, G the shear modulus, b the length of Burgers vector, k Boltzmann constant, T the temperature, d the mean grain diameter, and g and n the grain size and stress exponents, respectively. Since Arthenius equation holds for diffusion coefficient, it is useful to express temperature dependence of creep rate in the $\log[\varepsilon_s T d^g/(\delta-\delta_o)^n]$ vs. 1/T coordinates. Such relations are shown in Figs. 5 to 7 for alloy A and for both creep mechanisms in alloy B. It is clear that the Arthenius equation is fulfilled and thus the apparent activation energies can be estimated. For alloy A

$$Q_V = (112 \pm 13)\ \text{kJ/mol}$$

and for alloy B

$$Q_V = (136 \pm 10)\ \text{kJ/mol}$$

$$Q_{NV} = (162 \pm 20)\ \text{kJ/mol}$$

where, as above, the subscripts V and NV denote the viscous and non-viscous creep mechanisms, respectively.

4. Discussion

The viscous creep was observed in both alloys, its rate being proportional to the applied stress and to the reciprocal of the third power of the grain size. Apart from the threshold stress observed, these characteristics correspond to Coble creep, described by the equation /3/:

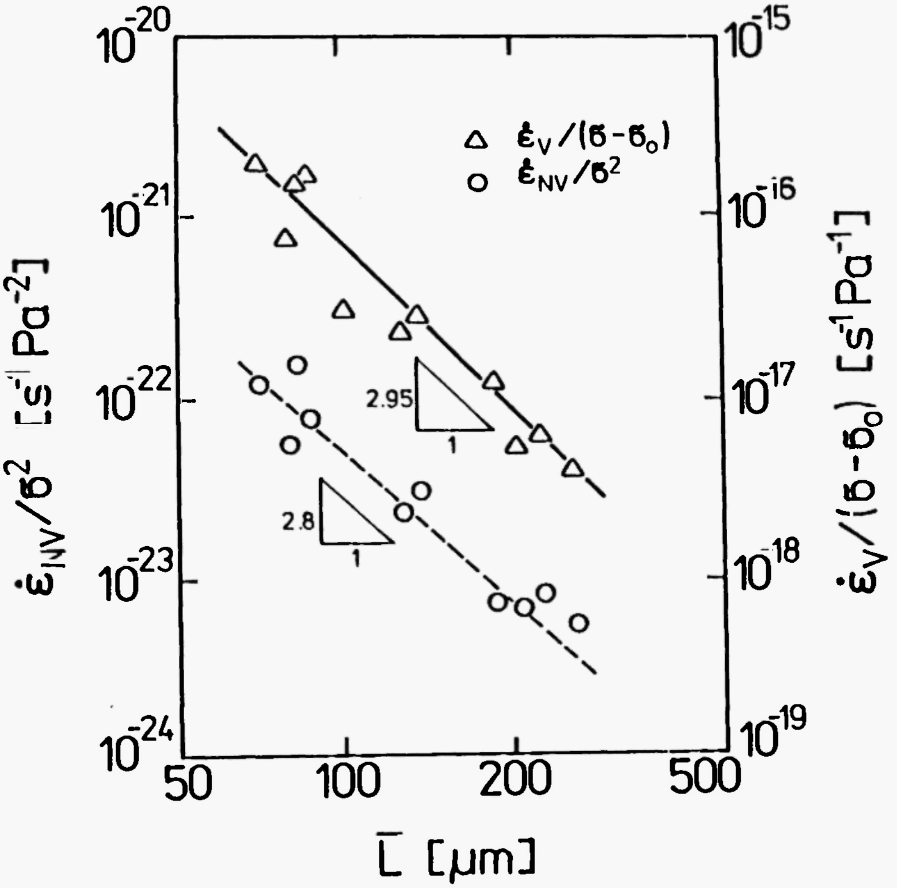

Fig. 4: Intercept grain size dependence of the $\dot{\varepsilon}_V/(\delta-\delta_o)$ and $\dot{\varepsilon}_{NV}/\delta^2$ products for alloy B at T = 773 K.

$$\dot{\varepsilon}_s = B_c \frac{D_B\delta_B\Omega}{d^3kT} \qquad (3)$$

where $D_B\delta_B$ is the grain boundary diffusional conductance, Ω the atomic volume and B_c the dimensionless constant. Assuming uniform spherical grains, the relations $B_c = 148/\pi$ and $d = 1.57\ \bar{L}$ hold. Cermák /4/ measured the grain boundary diffusional conductances in the alloys investigated in the present paper. Using his values of $D_B\ \delta_B$, the normalized creep rates were calculated by means of Eq. 3. The results of these calculations are compared with the experimental creep data in Figs. 5 and 6. It can be seen that experimental creep rates are by factors 4 and 3 higher than the calculated ones for alloys A and B, respectively. Similar or even larger differences were found for most of the experimental data on diffusional creep in pure metals /5,6/.

Until now, many attempts to explain such differences have been made; however, none of them has been generally accepted. We believe that among the possible reasons for the above differences the fact should be considered that while Coble Eq. 3 assumes spherical grains of uniform size, the structure of creep specimens is quite different. The strong influence of grain size and grain shape distributions on the diffusional creep rate is well-known /7,8/, but no method to account for measurable parameters of real structure has been published to date. The activation energy of grain boundary diffusion in alloy A reported by Cermák /4/, namely (125 ± 13) kJ/mol, is in good agreement with the measured apparent activation energy of viscous creep mechanism mentioned in the previous section. Since the activation energy of grain boundary diffusion in alloy B can be expected to be similar to that in alloy A, viscous creep in both alloys is controlled by grain boundary diffusion. Thus, the viscous creep mechanism in both alloys is without any doubt the Coble diffusional creep.

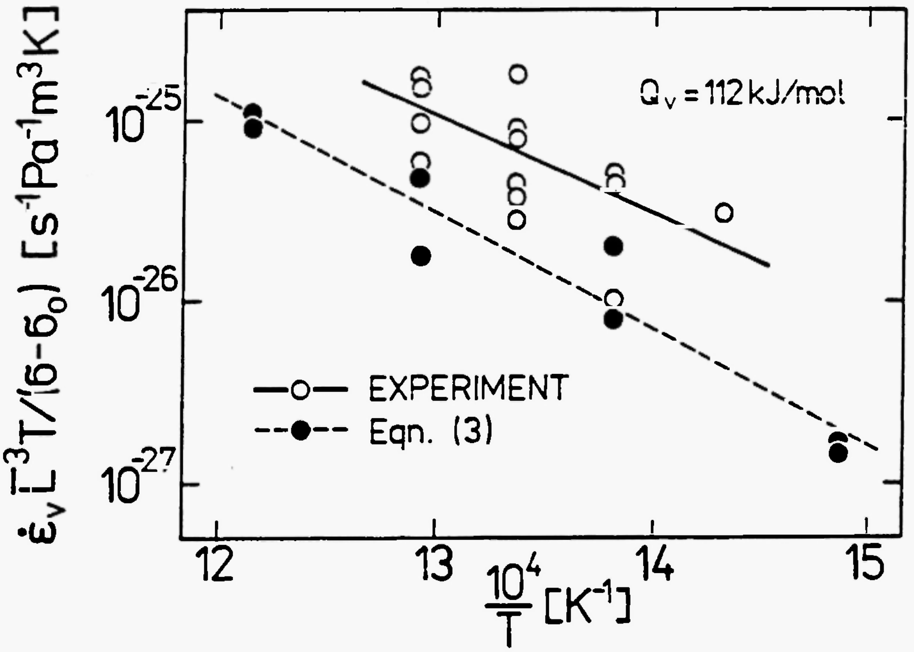

Fig. 5: Reciprocal temperature dependence of temperature and grain-size normalized product $\dot{\varepsilon}_V/(\delta-\delta_0)$ for alloy A.

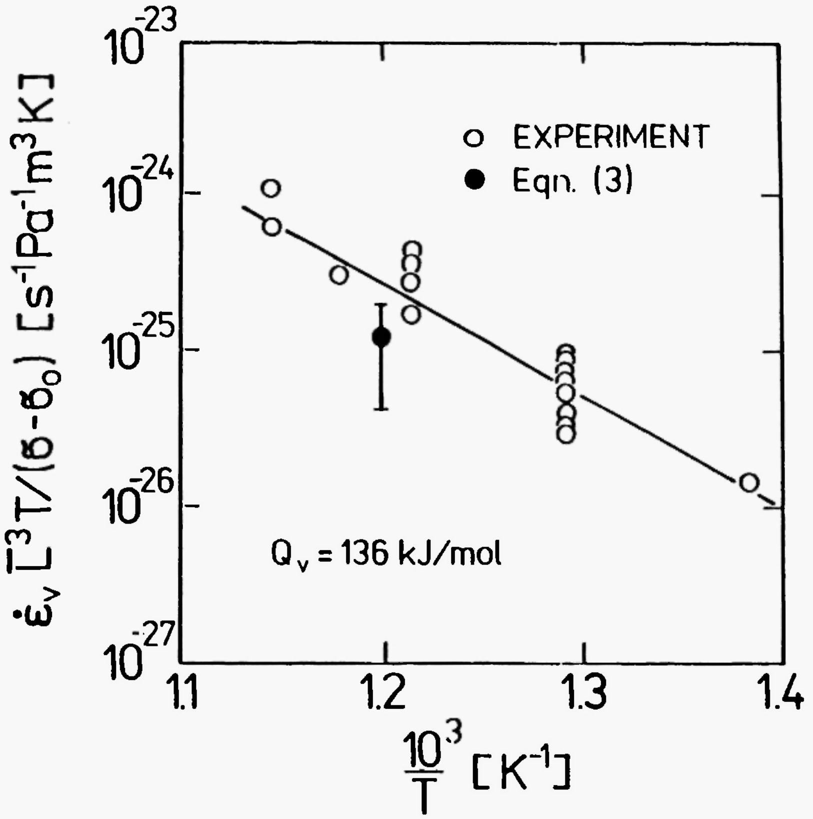

Fig. 6: Reciprocal temperature dependence of temperature and grain-size normalized product $\dot{\varepsilon}_V/(\delta-\delta_0)$ for alloy B.

The interpretation of the non-viscous mechanism in alloy B is not so straightforward. In fact, no contemporary model predicts a creep rate to be proportional to the second power of applied stress and to the reciprocal of the third power of grain size, though similar characteristics are frequently observed for straining in region II of superplasticity. Since the non-viscous creep mechanism operates in parallel with the Coble diffusional creep, it cannot be interpreted as another grain boundary controlled diffusional creep. On the other hand, the diffusional creep enhanced by grain boundary migration, as proposed by Chen /9/, must be taken into consideration. Though it is in principle viscous creep, the strong threshold behaviour of this mechanism may cause an apparent stress exponent higher than 1. Chen's creep is associated with large scale grain boundary migration; therefore, careful metallographic observations were made to obtain information on such migration. Since no grain boundary migration was detected, Chen's creep mechanism could be rejected. Another possible interpretation of the creep in question is offered by the mechanisms of grain boundary sliding accommodated by crystallographic slip in grain mantle. Mechanisms of this type are considered mostly as mechanisms of superplasticity. However, as mentioned above, the main characteristics of the above creep behaviour are the same as those of the superplastic ones. Some researchers, namely Gifkins /10/ and Ruano, Wadsworth and Sherby /11/, pointed out that there is no reason for superplastic mechanisms not to operate under creep conditions. Some theories of mechanisms of grain boundary sliding were published by Ball and Hutchinson /12/ and Gifkins /10/. These theories were further elaborated on by Sherby and Ruano /13/ and especially by Kaibyshev, Valiev and Emaletdinov /14/.

All of them predict the strain rate inversely proportional not to the third but to the second power of grain size. Accepting this grain size dependence of creep rate and following Kaibyshev et al. /14/, we can write

$$\dot{\varepsilon}_{ii} = \frac{D_B \delta_B\ G}{1.25\ kT} \left(\frac{b_B}{d}\right)^2 \left(\frac{\delta - \delta_B}{G}\right)^2 \tag{4}$$

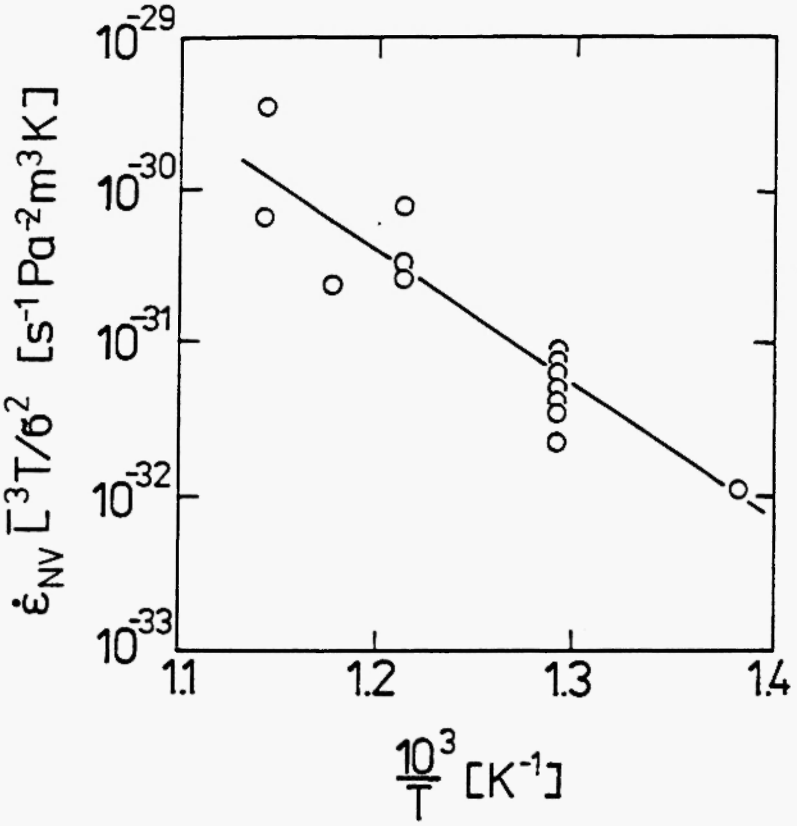

Fig. 7: Reciprocal temperature dependence of temperature and grain-size normalized product $\dot{\varepsilon}_{NV}/\delta^2$ for alloy B.

where b_B is the length of Burgers vector of grain boundary dislocation and δ_B the stress needed to activate lattice dislocation sources due to the stress concentrations generated by pile-ups of grain boundary dislocations. Correlation of the results of calculations with the experiment is illustrated in Fig. 8. It can be seen that the agreement between theory and experiment is almost as good as in the case of diffusional creep, provided $\delta_B = 0$. Thus, non-viscous creep seems to result from grain boundary sliding accommodated by crystallographic slip in narrow zones adjoining grain boundaries.

The reasons for why the non-viscous creep mechanism contributes to the measured creep rate in alloy B but not in alloy A remain to be elucidated. Because of the difference in the viscous creep rate scales with that in the grain boundary diffusional conductance, Eqs. 3 and 4 by themselves do not provide any explanation of such a different behaviour. Nevertheless, aluminium segregation to grain boundaries may affect their structure, which is supported by a significant difference in grain boundary diffusional conductances. Thus, the effective values of b_B can be different in both alloys. Moreover, a reduction of the non-viscous creep rate by a factor of about 0.5 could make the non-viscous creep undetectable in the measurements performed in the present work. Another possible explanation may consist in accommodating mechanisms as affected by the stacking fault energy. According to Howie and Swann /15/, the stacking fault energy of alloy A is about an order of magnitude higher than that of alloy B. Despite the possible effect of stacking fault energy on the grain boundary structure, the strengthening processes associated with accommodating dislocation slip may be different. The fact that the transient strain in alloy A is larger than that in alloy B /16/ supports the idea that such processes can inhibit non-

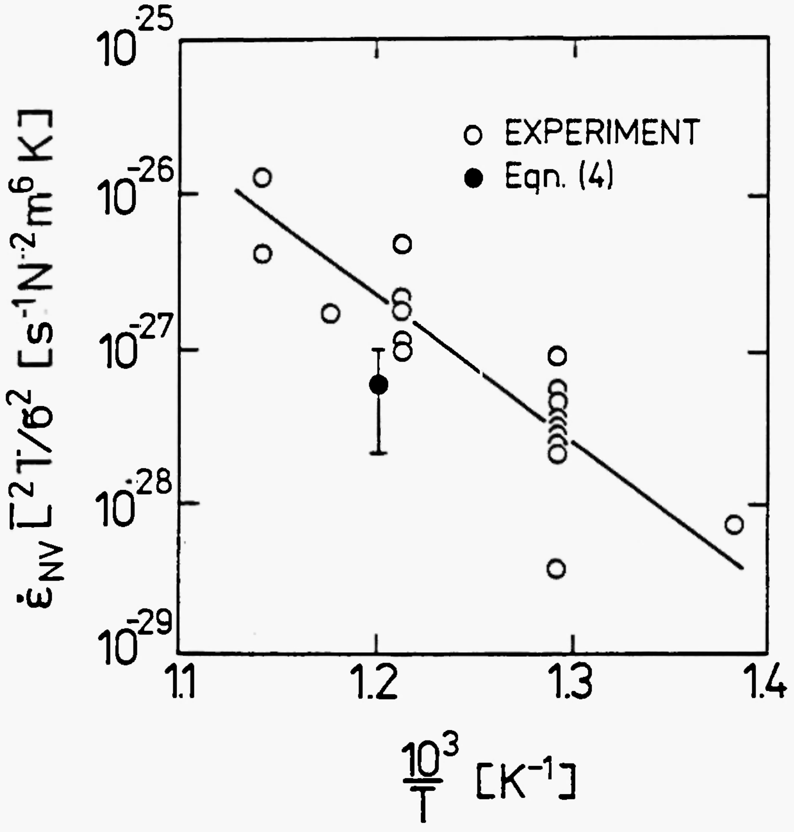

Fig. 8: Reciprocal temperature dependence of temperature and grain-size normalized product $\dot{\varepsilon}_{NV}/\delta^2$ for alloy B. ○ experimental data, ● data calculated from Eq. 4.

viscous creep mechanism in the course of the transient stage.

5. Conclusion

The creep in a Cu-5Al solid solution alloy (alloy A) at intermediate temperatures and low stresses is a result of the stress-directed diffusional transport of matter via grain boundaries (Coble creep). On the other hand, the creep in a Cu-14Al solid solution alloy (alloy B) results from two mechanisms operating in parallel, the first being viscous and the second non-viscous. The characteristics of the viscous mechanism - Coble creep - are the same in both alloys. The creep rate due to the non-viscous mechanism in alloy B varies with the second power of applied stress and the reciprocal of the third power of grain size. This result cannot be correlated with any of the models published to date. The model of grain boundary controlled diffusional creep as well as the model of diffusional creep enhanced by grain boundary migration can be excluded. The non-viscous creep mechanism is assumed to consist of grain boundary dislocation motion resulting in grain boundary sliding, accommodated by crystallographic slip in the narrow zones adjoining grain boundaries.

References

1. Fiala, J. and Cadek, J., *Metall. Mater.*, **20**, 277 (1982).
2. Kloc, L., Fiala, J. and Cadek, J., *Mater. Sci. Eng.*, **A130**, 61 (1990).
3. Coble, R.L., J. *Appl. Phys.*, **34**, 1679 (1963).
4. Cermák, J., *Phys. Status Solidi*, **A121**, K31 (1990).
5. Fiala, J., Novotny, J. and Cadek, J., *Mater. Sci. Eng.*, **60**, 195 (1983).
6. Mishra, R.S., Jones, H. and Greenwood, G.W., *Scripta Metall.*, **22**, 323 (1983).
7. Nix, W.D., *Metals Forum*, **4**, 38 (1981).
8. Schneibel, J.H., Coble, R.L. and Cannon, R.M., *Acta Metall.*, **29**, 1285 (1981).
9. Chen, I.-W., *Acta Metall.*, **30**, 1317 (1982).
10. Gifkins, R.C., *Metall. Trans.*, **A7**, 1225 (1976).
11. Ruano, O.A., Wadsworth, J. and Sherby, O.D., *Mater. Sci. Eng.*, **84**, LI (1986).
12. Ball, A. and Hutchinson, M.M., *Metal Sci. J.*, **3**, 1 (1969).
13. Sherby, O.D. and Ruano, O.A., in: Superplastic Forming of Structural Alloys, N.E. Paton and C.A. Hamilton (Eds.), Metallurgical Transactions of AIME, Warrendale, PA, 241 (1982).
14. Kaibyshev, O.A., Valiev, R.Z. and Emaletdinov, A.K., *Phys. Status Solidi*, A**90**, 197 (1985).
15. Howie, A. and Swann, P.R., *Philos. Mag.*, **6**, 1215 (1961).
16. Kloc, L., Fiala, J. and Cadek, J., in: Proc. of VIIIth International Symposium on Creep Resistant Metallic Materials, Publ. House of the Czech. Sci. Soc. Ceske Budejovice, Zlín Czechoslovakia, 314 (1991).